



A method for state of energy estimation of lithium-ion batteries based on neural network model

Guangzhong Dong, Xu Zhang, Chenbin Zhang, Zonghai Chen*

Department of Automation, University of Science and Technology of China, Hefei 230027, PR China

ARTICLE INFO

Article history:

Received 24 January 2015

Received in revised form

19 July 2015

Accepted 20 July 2015

Available online xxx

Keywords:

State of energy

Wavelet neural network

Lithium-ion batteries

Particle filter

ABSTRACT

The state-of-energy is an important evaluation index for energy optimization and management of power battery systems in electric vehicles. Unlike the state-of-charge which represents the residual energy of the battery in traditional applications, state-of-energy is integral result of battery power, which is the product of current and terminal voltage. On the other hand, like state-of-charge, the state-of-energy has an effect on terminal voltage. Therefore, it is hard to solve the nonlinear problems between state-of-energy and terminal voltage, which will complicate the estimation of a battery's state-of-energy. To address this issue, a method based on wavelet-neural-network-based battery model and particle filter estimator is presented for the state-of-energy estimation. The wavelet-neural-network based battery model is used to simulate the entire dynamic electrical characteristics of batteries. The temperature and discharge rate are also taken into account to improve model accuracy. Besides, in order to suppress the measurement noises of current and voltage, a particle filter estimator is applied to estimate cell state-of-energy. Experimental results on LiFePO₄ batteries indicate that the wavelet-neural-network based battery model simulates battery dynamics robustly with high accuracy and the estimation value based on the particle filter estimator converges to the real state-of-energy within an error of ±4%.

© 2015 Elsevier Ltd. All rights reserved.

1. Introduction

Due to consideration of energy crisis and environment protection, the low-emission and energy saving EV (electric vehicles) have become the developing tendency of the energy transformation. In recent years, various electrochemical energy storage systems have been introduced for EV applications, like NiMH (Nickel/Metal Hydride), Li-ion (Lithium-ion) batteries as well as other types such as ultra-capacitors and fuel cells etc. Li-ion batteries have become widely used power source in EVs for its high power density, high energy density and long lifetime. For instance, Zou et al. [1] proposed a combined SOC (state-of-charge) and SOH (state-of-health) estimation method over the lifespan of a Li-ion battery. Hu et al. [2] presented an integrated method for the capacity estimation and remaining useful life prediction of Li-ion battery. Kang et al. [3] proposed a method to compare the comprehensive properties of different battery systems in terms of a parameter, energy efficiency. Hu et al. [4] discussed an ameliorated

sample entropy-based capacity estimator for prognostics and health management of Li-ion batteries in electrified vehicles. Fathabadi et al. [5] presented a novel Li-ion battery pack design including hybrid active-passive thermal management system. In order to maintain optimum battery performance, a BMS (battery management system) is critical for battery system. Therefore, the BMS must know accurate and reliable battery system parameters. The SOC is a critical parameter for power battery systems. It plays a role in representing the residual energy of the battery in traditional applications. Thus, it is used to predict residual driving mileage of EVs. However, with the sophisticated and complex functional demand trend of BMS, the disadvantages of using the estimated SOC to represent the battery residual energy become more prominent [6]. The SOE (State of energy), which provides the essential basis of energy deployment, load balancing and security of electricity for the complex energy systems, is an important evaluation index for energy optimization and management of power battery systems [6].

Traditionally, SOC is used not only to protect battery from being over charged or over discharged, but also to represent the residual energy of battery. Nevertheless, there are several disadvantages of using the estimated SOC to represent the battery residual energy, as

* Corresponding author. Tel.: +86 055163606104..

E-mail address: chenzh@ustc.edu.cn (Z. Chen).

reviewed by Liu et al. [6]. Firstly, the SOC is defined as the ratio of the residual capacity to the total original capacity of a Li-ion battery, which means that SOC cannot indicate the energy state on which the battery application conditions is dependent. Some works have considered the residual available capacity instead of the SOC to determine the residual energy of battery. For instance, to the determination of the available energy stored in the battery, Waag et al. [7] employed the estimation of battery electromotive force to estimate SOC and capacity of the battery. Hausmann et al. [8] expanded the Peukert equation for battery capacity modeling through inclusion of a temperature dependency. Shen et al. [9] defined the state of available capacity, instead of SOC to denote the battery residual available capacity for lead-acid batteries. Liu et al. [10] proposed an extended Peukert equation to estimate the available capacity of batteries including the temperature effect. Secondly, the battery energy can be regarded as the product of the capacity and the OCV (open circuit voltage) of the battery. Although there is a positive correlation between battery SOE and SOC, they have no explicit quantitative. The SOC decreases linearly with the discharge current, but the battery energy is the product of the capacity and the OCV of the battery. Battery energy change has direct link with its real-time voltage, as a result, it is hard to be accurately calculated. Thirdly, the discharge current and the temperature which usually change dramatically due to the dynamic load in actual battery system will have significant effects on battery performance. Wang et al. [11] measured the electronic conductivity of LiFePO₄ and LiFePO₄/C at various temperatures to understand the difference of low-temperature electrochemical performance between the carbon-coated and uncoated LiFePO₄ cathodes. Yi et al. [12] reported a modeling methodology on the temperature dependence of discharge behavior of a Li-ion battery in low environment temperature. At the same SOC, the SOE may change on account of the fact that the discharge efficiency is dependent on the discharge current and temperature [6]. Thus, it is necessary to take the effect of discharge current and temperature into account for getting a more accurate SOE estimation.

In recent years, many researches have been devoted to developing improved methods for SOC estimation. Ng et al. [13] proposed a smart estimation method based on coulomb counting. The electrical model based methods established battery models to capture the relationship between the SOC and the OCV of the battery, then the adaptive filters, such as Kalman filter [14] and particle filter, for instance, dual-particle-filter presented in Liu et al. [15], unscented particle filter proposed in Zhong et al. [16] and He et al. [17]. Charkhgard et al. [18] presented a method for SOC estimation of Li-ion batteries using neural networks and the EKF (extended Kalman filter). Some works developed the fuzzy logic method [19] and support vector machines [20] for SOC estimation. Most of these methods have been widely used and made acceptable achievements in different applications. Adopting same methods as SOC estimations, an assortment of techniques have previously been reported to measure or estimate the SOE of the cells. Among them, Stockar et al. [21], Mamadou et al. [22] and Kermani et al. [23] presented the definition of SOE and the algorithms to follow-up the SOE based on direct power integral method which used power integral to estimate the SOE. However, this method had a significant estimation error because of the measurement noises of current and terminal voltage of the battery. Liu et al. [6] has proposed an improved direct SOE estimation method at dynamic current and temperature conditions based on BPNN (back-propagation neural network). In the input layer, the battery terminal voltage, the current and the temperature are taken as the input parameters, and the output layer is the estimated SOE. However, this method is an open-loop estimation so that its estimation accuracy becomes poor due to the incorrect measurements. Wang

et al. [24] has proposed a joint estimator for SOC and SOE to overcome the disadvantages of power integral method. However, the SOE estimation accuracy depends on the SOC estimation accuracy in this developed method. Zhang et al. [25] proposed a novel model-based joint estimation approach to improve the estimation accuracy and reliability for battery SOE and power capability, and the battery model takes SOE as a state variable. However, it has not taken the influence of temperature and discharge rate on total available energy into account, while the total available energy is a critical parameter directly limit the pack performance through "capacity fade". Unlike SOC, SOE is integral result of battery power, which is the product of current and terminal voltage. On the other hand, like SOC, SOE has an effect on terminal voltage. Therefore, it is hard to solve the nonlinear problems between SOE and terminal voltage, which will complicate the estimation of a battery's SOE. Therefore, there is need to establish a battery state space model that takes SOE as a state variable. Once this model is established, the adaptive filter algorithms used in SOC estimation will be available for SOE estimation for getting more accurate SOE estimation.

In this paper, a WNN (wavelet neural network)-based battery state-space model and PF (particle filter) estimator is carried out to improve the battery modeling and SOE estimation. It is organized as follows. A clear scheme of battery test bench, the definition of SOE and some battery test data analysis for Li-ion batteries are given in Section 2. The test results are used to analyze some influencing factors of the SOE estimation, such as OCV, discharge current and temperature. In Section 3, a state-space model of the SOE that takes into account the effect of the discharge current and temperature is established. Then, parameters of the WNN-based battery model are identified by the experimental data of LiFePO₄ batteries. In Section 4, the PF method based on the proposed model is applied to estimate the SOE. In Section 5, simulations and comparison tests based on the proposed model and real battery data will be presented to verify the superiority of the proposed algorithm.

2. Experimental

As an application case, LiFePO₄ batteries are chosen to verify the proposed approach. Section 2.1 gives a brief introduction for the test bench. In order to analyze the characteristics of SOE, the definition of SOE is first given in Section 2.2.1. Then, the test data analysis is given in Section 2.2.2.

2.1. Test bench

Experimental studies are conducted on LiFePO₄ batteries with a rated capacity of 9 Ah (produced by Hefei Guoxuan High-Tech Power Energy CO., Ltd. of China). The parameters of the battery are given in Table 1. In order to acquire experimental data such as current, voltage and temperature, a battery test bench has been established. The configuration of the test bench is drawn in Fig. 1, which consists of a battery test system NEWWARE BTS4000, a BMS, a CAN communication unit, a programmable temperature chamber, a computer to program and store experimental data and some test cells. The NEWWARE BTS4000 is responsible for loading the

Table 1
Battery parameters of LiFePO₄.

Parameter	Value
Rated capacity	9 A h
Low cutoff voltage	2.0 V
Upper limit voltage	3.65 V
Operating temperature	-20° ~ 60 °C

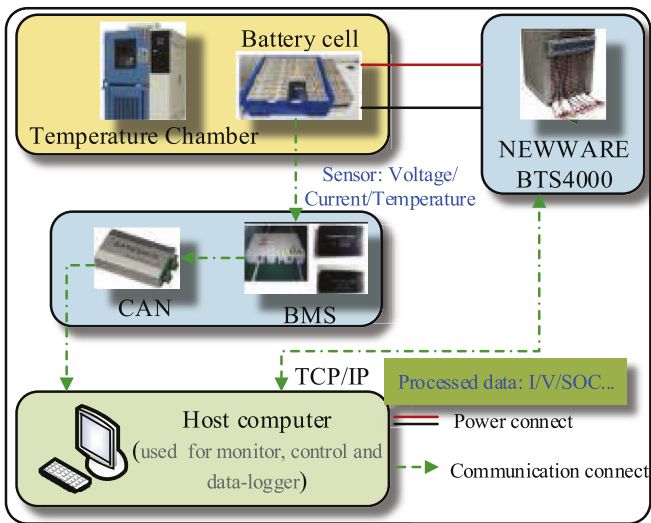


Fig. 1. Battery test bench.

currents or powers profiles on the test cells with the voltage limits of 0–5 V and a current limits of ± 100 A. The voltage and current measurement accuracy is $\pm 0.1\%$. The experimental data such as current, voltage, temperature and accumulative AH (ampere-hour) are measured by the NEWWARE BTS4000 and stored in the host computer. The BMS and CAN communication unit perform the function of battery protection and transmit the data of fault information to the host computer. The programmable temperature chamber provides manageable temperature for battery. All the experimental data are collected with a PC software, and used as inputs for MATLAB.

2.2. The definition of SOE and test data analysis

2.2.1. SOE

The SOE provides the information of the remaining available energy of Li-ion batteries. In this study, the SOE is defined as the ratio of the residual energy to the total original energy capacity of a Li-ion battery. It can be expressed as following equation [26]:

$$SOE(t) = SOE(t_0) - \frac{\int_0^t P(\tau)d\tau}{E_N} \quad (1)$$

where $SOE(t)$ is the SOE at time t ; $SOE(t_0)$ is the SOE at time t_0 ; E_N is the nominal total energy of the battery. $P(\tau)$ is the effective power at τ (assumed positive for discharge, negative for charge).

2.2.2. Test data analysis

In order to identify the OCV at different SOC, a test is performed on LiFePO₄ batteries. The test scheme is designed as follows: the battery is first discharged by a 10% of the nominal capacity from fully charged state at preset current. Then, it is left in open-circuit state and the terminal voltage is monitored simultaneously. The measured terminal voltage is considered to reach a real OCV after 3 h until the change of the terminal voltage is insignificant. The battery is continuously discharged by a further 10% of the nominal capacity at the same current. The above scheme is performed repeatedly until the battery reaches the low cutoff voltage in Table 1. The OCV results are plotted in Fig. 2.

According to Fig. 2, the OCV drops quickly as the SOC approaches 0% and rises quickly as SOC reaches around 100%. The OCV is a nonlinear function of SOC. Thus, the discharged energy of the

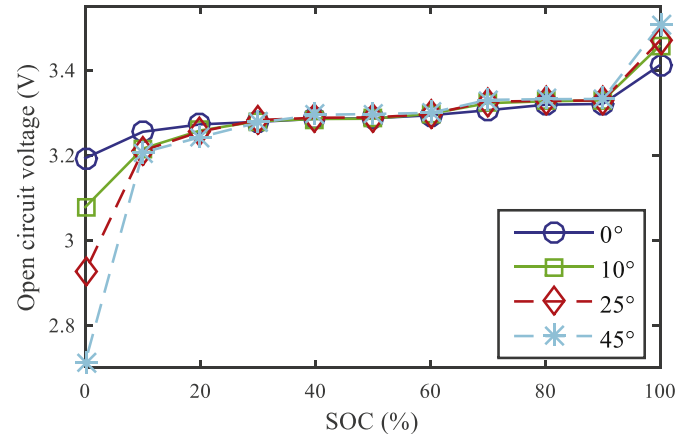


Fig. 2. OCV curves under different temperatures.

battery is not a constant at the same interval of the SOC, which means SOE is not a linear function of SOC. Furthermore, in order to illustrate this, the discharged energy at a 10% interval of the SOC from 100% to 0% is plotted in Fig. 3. According to Fig. 3, in a certain range of temperature, with the rise of temperature, the discharged energy shows a rise trend. At the same temperature, with the decrease of SOC, the discharged energy shows a decrease trend. Therefore, the SOC is different to the SOE. It cannot represent the residual energy of battery accurately.

The temperature and discharge current can influence the total available energy of the battery. The discharged energy of the battery with various current at different temperature is plotted in Fig. 4. According to Fig. 4, in a certain range of temperature, with the rising temperature, the total available energy presents a significant increase at the same discharge rate. And total available energy shows a decreasing trend with the increasing discharge rate at the same temperature. The discharged energy of the battery is greatly related on the discharge efficiency which varies with the discharge currents and temperatures [6]. Therefore, it is necessary to establish a battery model that takes into consideration the effects of temperature and discharge rate for the accurate SOE estimation.

3. Modeling

3.1. New model of the total available energy

The total available energy is an important parameter of state-space model. Generally, the total available energy can be regarded

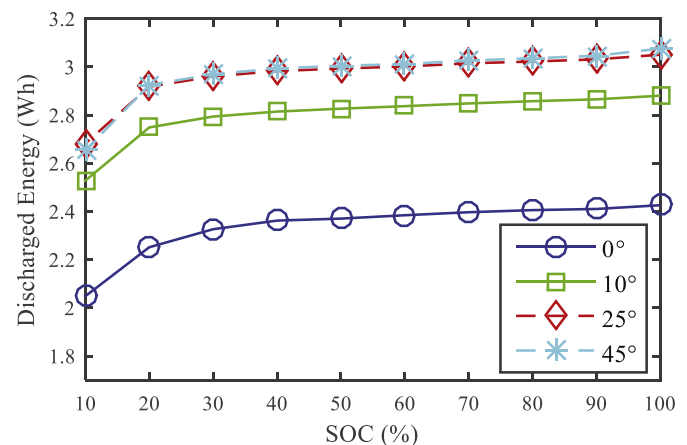


Fig. 3. The discharged energy at different SOC and temperature.

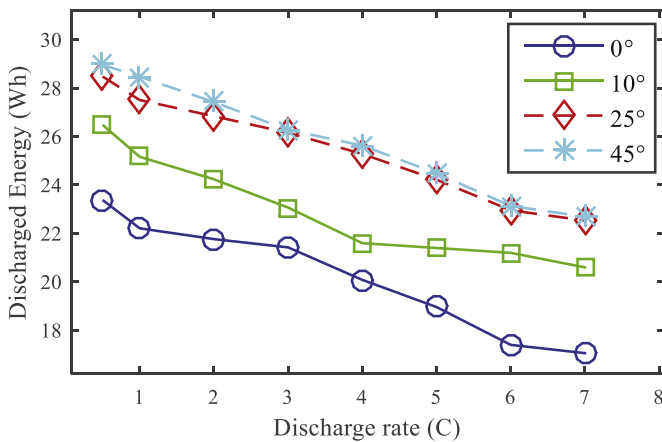


Fig. 4. The discharged energy at different currents and temperatures.

as the product of total available capacity and $OCV_{SOC=100\%}$. Fig. 5 shows that the total available capacity of the Li-ion battery changes along with the temperature and discharge rate. Fig. 5(a) shows that the total available capacity is essentially unchanged at the same discharge rate at normal temperature, while the variability of the total available capacity is very large at low temperature. Fig. 5(b) shows that the total available capacity is inversely proportional to the discharge rate. The total available capacity $C_n(T, \kappa)$ is a function of the temperature and the discharge rate. The total available capacity of the battery is inversely proportional to the discharge rate at normal temperature (from 15 °C to 45 °C), while the total available capacity is mainly determined by the temperature at low temperature. Refer to He et al. [17], the empirical expression of $C_n(T, \kappa)$ can be described by Eq. (2),

$$C_n(T, \kappa) = \begin{cases} C_n + a/\kappa, & (T > T_0, \kappa > \kappa_0) \\ C_n + a/\kappa_0, & (T > T_0, \kappa \leq \kappa_0) \\ b\Delta T^2 + c\Delta T + C_n + a/\kappa & (T \leq T_0, \kappa > \kappa_0, \Delta T = T - T_0) \\ b\Delta T^2 + c\Delta T + C_n + a/\kappa_0 & (T \leq T_0, \kappa \leq \kappa_0, \Delta T = T - T_0) \end{cases} \quad (2)$$

where C_n is nominal capacity of the battery; T is temperature; $\kappa = |i|/C_n$ is discharge rate; $\{a, b, c\}$ are constants obtained by the experiment data.

Theoretically, $OCV_{SOC=100\%}$ does not correlate with discharge rate, while $OCV_{SOC=100\%}$ changes along with temperature linearly in a certain range of temperature [15], as shown in Fig. 6. The fitting function of the curve is shown as Eq. (3). Thus, the empirical

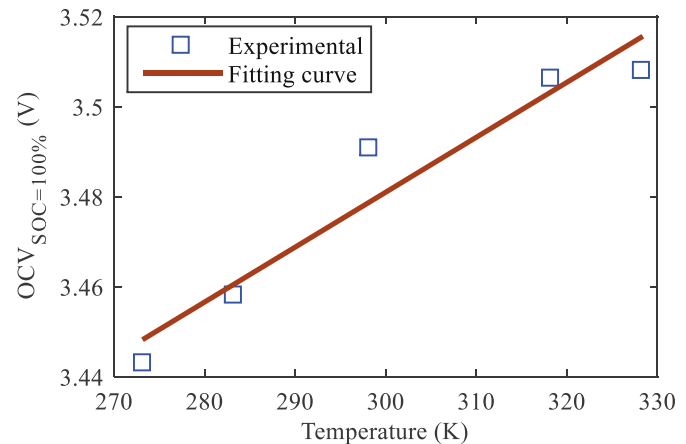


Fig. 6. $OCV_{SOC=100\%}$ changes along with environment temperature.

expression of the total available energy $E_N(T, \kappa)$ can be described by Eq. (4).

$$OCV_{SOC=100\%}(T) = \alpha T + \beta \quad (3)$$

$$E_N(T, \kappa) = C_n(T, \kappa) \cdot OCV_{SOC=100\%}(T) \quad (4)$$

3.2. SOE as a state-space variable

The SOE is defined as Eq. (1). To estimate the SOE by PF algorithms, the discrete time state-space equation must be available. The discrete time state-space equation of Eq. (1) is shown as Eq. (5),

$$SOE(k) = SOE(k-1) - \frac{\eta I_{k-1} V_{k-1} \Delta t}{E_N(T, \kappa)} \quad (5)$$

where η is Coulombic efficiency; I_{k-1} and V_{k-1} are current and terminal voltage at sample time $k-1$, respectively. Δt is the sample time. $E_N(T, \kappa)$ is the total available energy.

3.3. Model measurement equation

The SOE of batteries has a nonlinear relationship with its terminal voltage, current and temperature. It is not an easy task to obtain this nonlinear relationship. One direct method to find this relationship is to analyze the chemical reaction equations, which is very complicated.

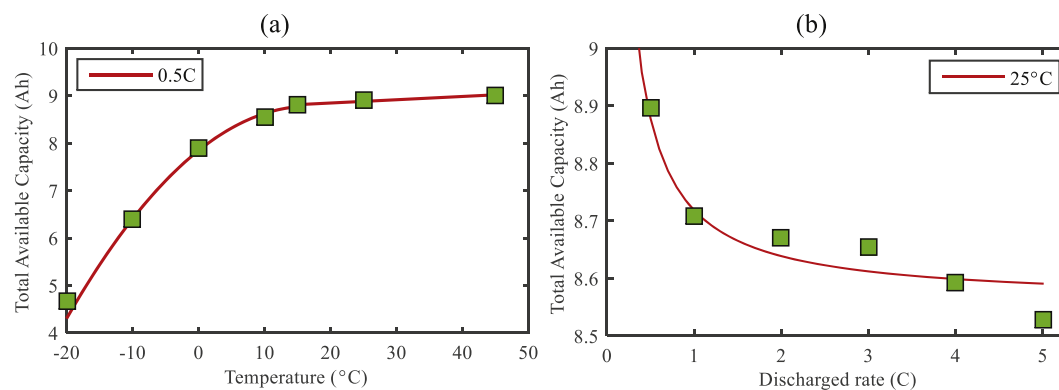


Fig. 5. The total available capacity changes along with: (a) environment temperature; (b) discharge rate.

Some works propose the electrical models of batteries using resistances and capacitances [25]. As a result, in these battery models, the governing differential equation between the voltage and current is of the first order. Therefore, in the discrete model, it is reasonable to consider the battery terminal voltage at the sample time k as a nonlinear function of the voltage at the sample time $k-1$ and the current, the SOE, temperature at sample time k .

ANNs are universal approximators and can approximate any nonlinear function with desired accuracies [18]. WNN is one of the most widely used networks, which has a good prediction performance [27]. Therefore, WNN is used to find the nonlinear model in this paper. Fig. 7 shows the structure of a WNN, where the inputs are the battery voltage at the sample time $k-1$ and the estimated SOE, the terminal current, and temperature at sample time k . The output is the battery voltage at the sample time k . It should be noted that all input and output variables of the WNN are normalized.

According to Fig. 7, the input vector of the input layer is $\mathbf{r}_k = [\text{SOE}_k, i_k, T_k, v_{k-1}]^T$, and the output vector of the output layer is $\mathbf{Y}_k = [v_k]^T$. S is the number of neurons in the hidden layer. The activation functions of neurons f^1 in the hidden layer is Morlet wavelet function, as shown in Eq. (6),

$$\psi(x) = \cos(1.75x)\exp(-0.5x^2) \quad (6)$$

The wavelet dilation parameter s and translation parameter t are given in Eq. (7),

$$\psi(s_i, t_i) = \cos\left(1.75 \frac{x - t_i}{s_i}\right) \exp\left[-0.5\left(\frac{x - t_i}{s_i}\right)^2\right] \quad (7)$$

Thus, the output of this WNN is the sum of the weighted Morlet wavelet functions as shown in Eq. (8),

$$F(\mathbf{r}_k) = \mathbf{b}^2 + \mathbf{LW}^{2,1}\psi(\mathbf{IW}^{1,1}\mathbf{P} + \mathbf{b}^1 + \mathbf{IW}^{1,2}v(k-1)) \quad (8)$$

where $\mathbf{r}_k = [\mathbf{P}^T, v_{k-1}]^T$, $\mathbf{P} = [\text{SOE}_k, i_k, T_k]^T$. The weight vectors $\{\mathbf{IW}^{1,1}, \mathbf{IW}^{1,2}, \mathbf{LW}^{2,1}, \mathbf{b}^1, \mathbf{b}^2\}$ and wavelet parameters $\{s, t\}$ are the free parameters of this network, and they can be defined during the training phase of the network using Back-Propagation algorithms.

3.4. Proposed model

Considering the SOE at the sample time k and the battery terminal voltage at $k-1$ as the state variables, the state vector is defined as Eq. (9),

$$\begin{aligned} X_k &:= \begin{bmatrix} x_1(k) \\ x_2(k) \end{bmatrix} = \begin{bmatrix} \text{SOE}(k) \\ v(k-1) \end{bmatrix} \\ \Rightarrow X_{k+1} &= \begin{bmatrix} x_1(k+1) \\ x_2(k+1) \end{bmatrix} = \begin{bmatrix} \text{SOE}(k+1) \\ v(k) \end{bmatrix} \end{aligned} \quad (9)$$

where v represents the terminal voltage. By using the aforementioned definition, the state-space model can be defined as Eq. (10),

$$\begin{aligned} \begin{bmatrix} x_1(k+1) \\ x_2(k+1) \end{bmatrix} &= \underbrace{\begin{bmatrix} x_1(k) - \frac{\eta_i \Delta t_i x_2(k)}{E_n(T, \kappa)} \\ F(\mathbf{r}_k) \end{bmatrix}}_{f(X_k, i_k, T_k)} + \begin{bmatrix} \omega_1(k) \\ \omega_2(k) \end{bmatrix} \\ y(k) &= \underbrace{x_2(k)}_{g(X_k, i_k, T_k)} + v(k) \end{aligned} \quad (10)$$

process noise
measure noise

where $F(\mathbf{r}_k)$ is the nonlinear function, which will be approximated by the WNN. $\{\omega(k)\}$ and $\{v(k)\}$ are the process and the measurement noises, respectively, with known pdfs: $\omega_1(k) \sim N(0, Q_1)$, $\omega_2(k) \sim N(0, Q_2)$, $\omega \sim N(\mathbf{0}, \mathbf{Q})$, $v_1(k) \sim N(0, R)$ and $R = \text{diag}\{Q_1, Q_2\}$.

The WNN based state-space model presented above is improved in three ways: (1) It considers the nonlinear relationship between SOE and terminal voltage, and the residual energy of the batteries is represented by SOE instead of SOC. (2) It considers the effect of the temperature and the discharge rate on the total energy, so it can describe the environmental factors more accurately. (3) It is an effective solution to the nonlinear problem between SOE and terminal voltage, which is modeled by WNN. These improvements of the proposed model will be verified in Section 5.1 through the simulation.

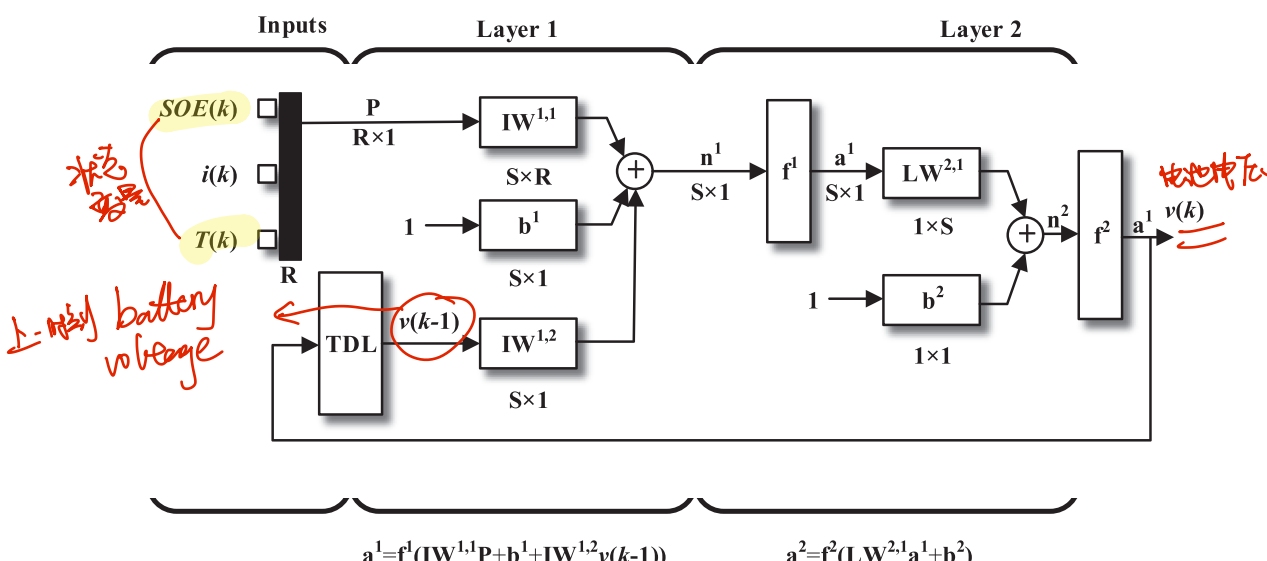


Fig. 7. Wavelet neural network structure of three layers: TDL is transmission delay layer.

Table 2

The parameters of the total available energy.

Parameter	Value
κ_0	0.33 h ⁻¹
T_0	288.15 K
C_n	8.707 Ah
a	0.1596 A
b	-0.0026 Ah K ⁻²
c	0.0284 Ah K ⁻¹
α	0.0012 V K ⁻¹
β	3.113 V

3.5. Model parameters identification

3.5.1. Identification of the total available energy

To improve the model accuracy under practical conditions, the parameters of the total available capacity is identified by applying the least squares method with the test data of the LiFePO₄ batteries. The results are given in Table 2.

3.5.2. Identification of the WNN

In order to acquire battery data to train the WNN based model, the CC (constant-current) and CV (constant-voltage) protocol is

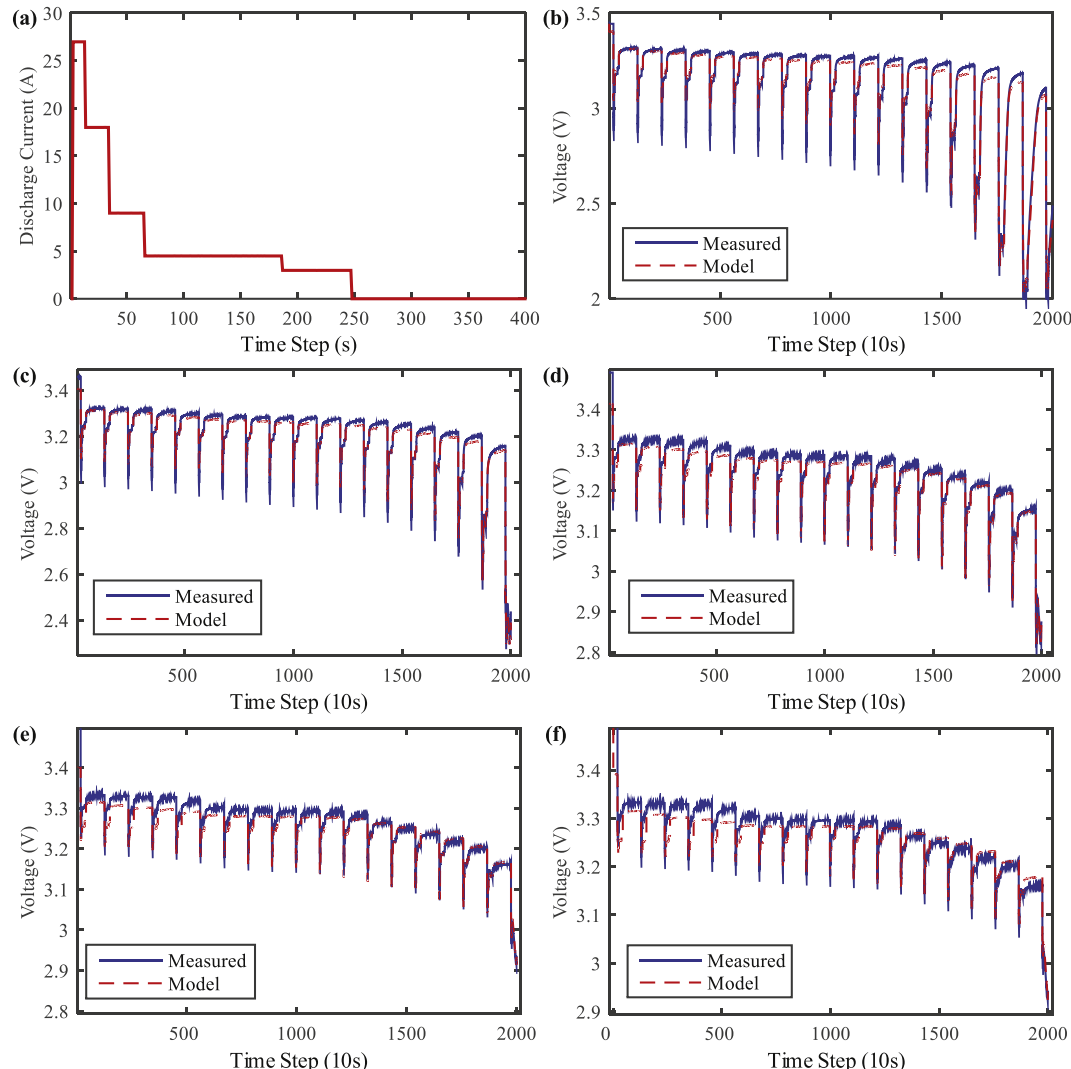


Fig. 8. Dynamic current conditions and comparison between model and measured voltage under different temperature conditions: (a) Dynamic current conditions, (b) 0 °C, (c) 10 °C, (d) 25 °C, (e) 45 °C, (f) 55 °C.

used to charge the battery, firstly. Then, the LiFePO₄ batteries are loaded with dynamic discharge currents at different temperatures, which are selected in [0 °C, 10 °C, 25 °C, 45 °C, 55°C]. The scheme of discharge current at each selected temperature points is shown in Fig. 8(a). The WNN based model is trained on the basis of the difference between the output value and the actual value of the terminal voltage. The target error of the WNN training is given by the MSE (mean square error), as shown in Eq. (11).

$$E_{mse} = \frac{1}{L} \sum_{p=1}^L (v_r(p) - v_e(p))^2 \quad (11)$$

where E_{mse} is the MSE between the estimated and the actual terminal voltage, L represents the number of the training data, $v_r(p)$ represents the actual voltage of the training data group p and $v_e(p)$ represents the estimated voltage by the WNN based model.

4. SOE estimation based on the PF

The PF methods have become a popular class of algorithms for solving the estimation problems of non-linear and non-Gaussian state space models [24]. To make the state estimator more

Table 3

Algorithm of particle filter.

Step 1	Initialization: $k = 0$ Randomly generate N initial particles on the basis of the pdf $p(\mathbf{X}_0)$. These particles are denoted by \mathbf{X}_0^i ($i = 1, 2, \dots, N$).
Step 2	<p>For $k = 1, 2, \dots$</p> <p>(a) Particle updates Generate N particles \mathbf{X}_k^i according to Eq. (10) and the last sampled N particles \mathbf{X}_{k-1}^i, $\mathbf{X}_k^i = f(\mathbf{X}_{k-1}^i, i_{k-1}) + \omega_{k-1}$.</p> <p>(b) Importance sampling step According to measurement y_k, calculate the maximum likelihood q_i of the particles \mathbf{X}_k^i as follows:</p> $q_i = p(y_k \mathbf{X}_k^i)$ $= p[y_k - g(\mathbf{X}_k^i, i_k, T_k)]$ $= \frac{1}{\sqrt{2\pi R}} \exp \left\{ - (y_k - g(\mathbf{X}_k^i, i_k, T_k))^2 \frac{1}{2R} \right\}$ <p>(c) Normalize the importance weights as follows $\bar{q}_i = q_i / (\sum_{j=1}^N q_j)$</p> <p>Now a set of posteriori particles \mathbf{X}_k^i can be generated on the basis of the weights \bar{q}_i by multinomial resampling method, $i = 1, 2, \dots, N$</p> <p>(d) Output The state variables after completion of the algorithm is $\mathbf{X}_k = \sum_i \bar{q}_i \mathbf{X}_k^i$</p>

concrete, the discrete time state-space models are used to describe the system information. For the discrete-time state-space model given in Eq. (10), the SOE estimation algorithm based on the PF is summarized as Table 3. The accuracy and robustness of the proposed method will be verified in Section 5.2.

5. Simulations and experimental results

To verify the WNN based model and the SOE estimation algorithm based on the PF, experiments and simulations are performed. Firstly, the performance of the WNN under dynamic current and constant temperature and constant current and dynamic temperature conditions is verified. Then, the superiority of PF method based on the WNN based model under constant current – dynamic temperature and dynamic current dynamic current – dynamic temperature conditions is verified through the comparison with power integral method which calculates the SOE according to Eq. (1) without PF filter.

5.1. The validation of the WNN based model

The training data of WNN based model is obtained under constant temperature conditions and dynamic current whose profile is plotted in Fig. 8(a). To verify to training results, the comparison results of the actual and the estimated voltage at each selected temperature ([0 °C, 10 °C, 25 °C, 45 °C, 55°C]) are plotted in Fig. 8(b)–(f), respectively. The numerical results are shown in Table 4. The WNN based model can simulate battery characteristics well at each selected temperature. Particularly, The RMSE (Root mean square error) is 16.2 mV, and the maximum absolute error is 78 mV at room temperature. The above results show that the WNN based model has been well trained.

Table 4

Training numerical results of WNN.

Temperature °C	Training numerical results of model	
	MaxAE ^a (V)	RMSE ^b (V)
0	0.2358	0.0316
10	0.1077	0.0172
25	0.0780	0.0162
45	0.1055	0.0190
55	0.1175	0.0201

^a MaxAE = Maximum Absolute Error.

^b RMSE = Root Mean Square Error.

The temperature usually changes dramatically in the battery system during the actual operation. To verify the performance of WNN based model under various temperatures, the battery is discharged at a constant rate 0.5 °C and the temperature rise from 0 °C to 60 °C. The change of temperature is shown in Fig. 9(a). The comparison results of the estimated and the actual voltage is shown in Fig. 9(b). The estimated and actual voltage curve lie together in a large range. The RMSE is 10.1 mV. The results show that the WNN based model has a good prediction performance.

The above comparison results show that the proposed WNN based model provides a good prediction performance. To suppress the system noises and improve the estimation accuracy, it is necessary applying the adaptive filter to the SOE estimation. The estimation algorithm, in this paper, is based on the PF.

5.2. SOE estimation algorithm verification

The voltage acquisition circuit in the BMS may inevitably produce measurement noise during the actual operation. The good estimation accuracy of the PF method is verified by comparing the performance of the power integral (without PF filter) and PF methods. The estimation results with dynamic current at different temperatures are used to verify the robustness of the proposed method. Herein, the SOE reference is the true value which is calculated without measurement noises.

Firstly, the temperature usually changes dramatically in the battery system during the actual operation. The battery is discharged with a constant rate 0.5 °C at different temperature conditions which are set at [0 °C, 10 °C, 25 °C, 45 °C, 55°C] and a dynamic temperature rising from 0 °C to 60 °C. The change of dynamic temperature is shown in Fig. 9(a). The comparison results of the SOE estimated by power integral method and PF method at different temperature conditions are shown in Fig. 10(a)–(f), respectively. The numerical results are shown in Table 5. According to Fig. 10, when the terminal voltage contains a measurement error, the SOE estimation results using the power integral method will produce relatively large oscillation and may deviate from the actual value, while the results using the PF method have a relatively good accuracy. Particularly, at the room temperature and variant temperature conditions, the RMSEs of the power integral method are 6.95% and 1.89% respectively, while the RMSEs of the PF method are 1.12% and 0.35% respectively. The maximum absolute SOE estimation errors are 10.5% and 4.5% for power integral method and 3.61% and 0.81% for PF method respectively. These results show that the PF method has a significant improvement than the power integral

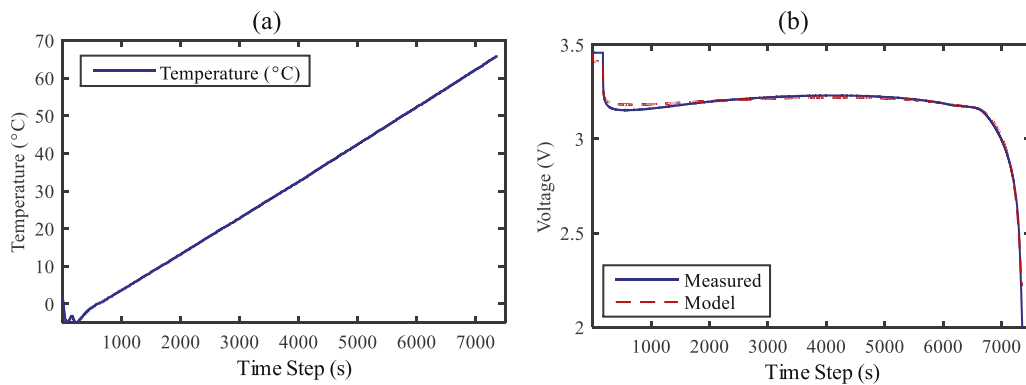


Fig. 9. Validation under constant current and dynamic temperature: (a) Dynamic temperature conditions; (b) Model voltage vs. measured.

method at different temperature conditions. The comparison results also show that the proposed WNN–PF based SOE estimation method can suppress the measurement noises and provide a better estimation accuracy than the power integral method.

Secondly, during the actual operation, not only the temperature in the battery system changes, the terminal current of the batteries will also vary dynamically. The battery is loaded under the current conditions in Fig. 8(a) at different temperature conditions which

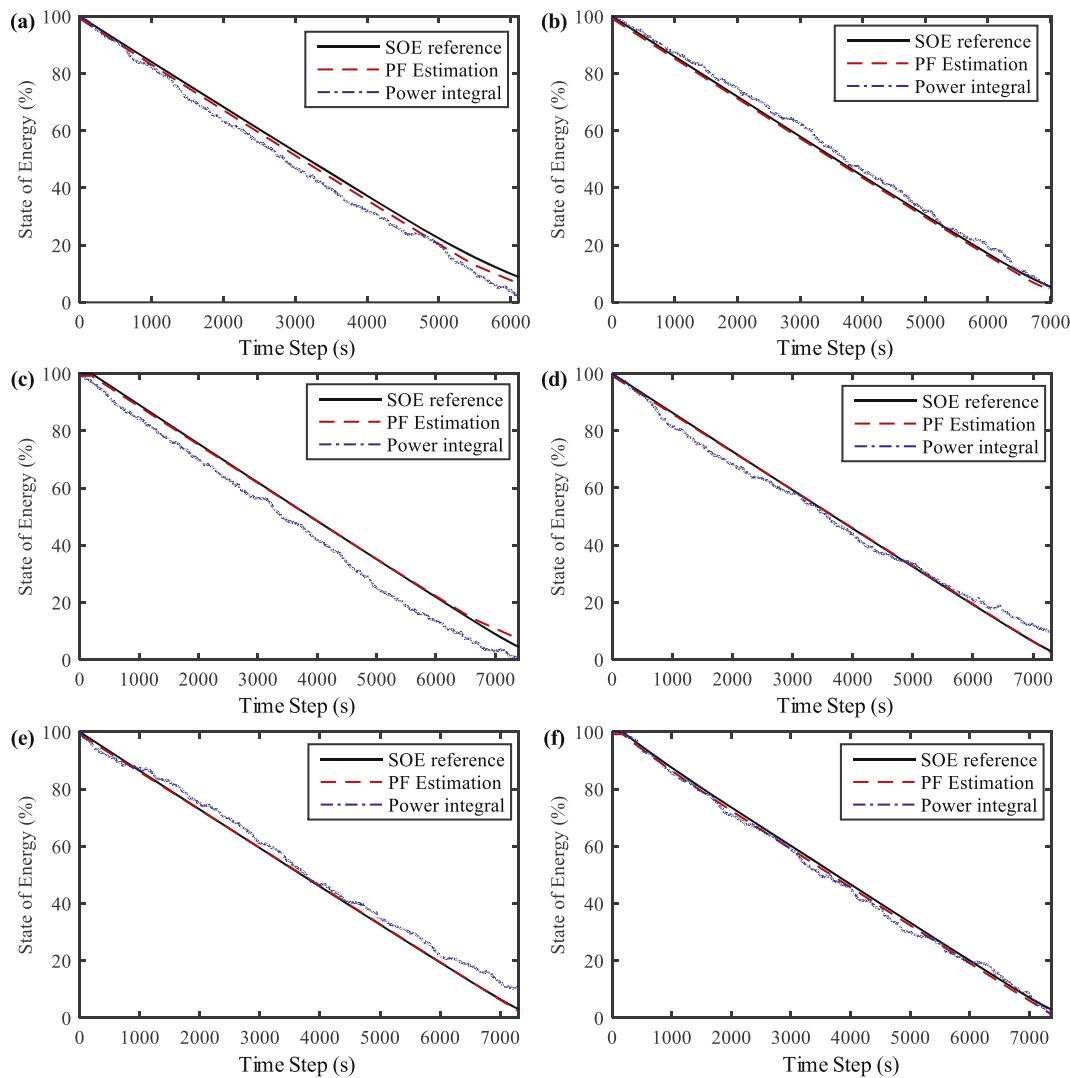


Fig. 10. SOE estimation results at different temperature conditions and constant discharge current after energy counting and PF filtering: (a) 0 °C, (b) 10 °C, (c) 25 °C, (d) 45 °C, (e) 55 °C, (f) dynamic temperature.

Table 5

Comparison of SOE estimation under constant current using PF and power integral approach.

Temperature(°C)	RMSE (%)		MaxAE (%)	
	Power integral	Particle filter	Power integral	Particle filter
0	4.43	0.85	6.99	1.86
10	2.31	0.91	4.97	1.03
25	6.59	1.12	10.5	3.61
45	3.21	1.21	7.10	1.43
55	3.24	0.78	7.47	1.01
Dynamic temperature	1.89	0.35	4.54	0.81

are set at [0 °C, 10 °C, 25 °C, 45 °C, 55 °C] and a dynamic temperature rising from 0 °C to 60 °C. The change of dynamic temperature is shown in Fig. 9(a). The comparison results of the SOE estimated by power integral method and PF method at different temperature conditions are shown in Fig. 11(a)–(f), respectively. The numerical results are shown in Table 6. According to Fig. 11, when the terminal voltage contains a measurement error, the SOE estimation results using the power integral method will also produce relatively large oscillation and may deviate from the actual value, while the results

using the PF method have a relatively good accuracy. Particularly, at the room temperature and dynamic temperature conditions, the RMSEs of the power integral method are 6.92% and 5.93% respectively, while the RMSEs of the PF method are 1.21% and 1.05% respectively. The maximum absolute SOE estimation errors are 12.3% and 11.1% for power integral method and 1.34% and 1.61% for PF method respectively. These results show that the PF method has a significant improvement than the power integral method at different temperature conditions. The comparison results also

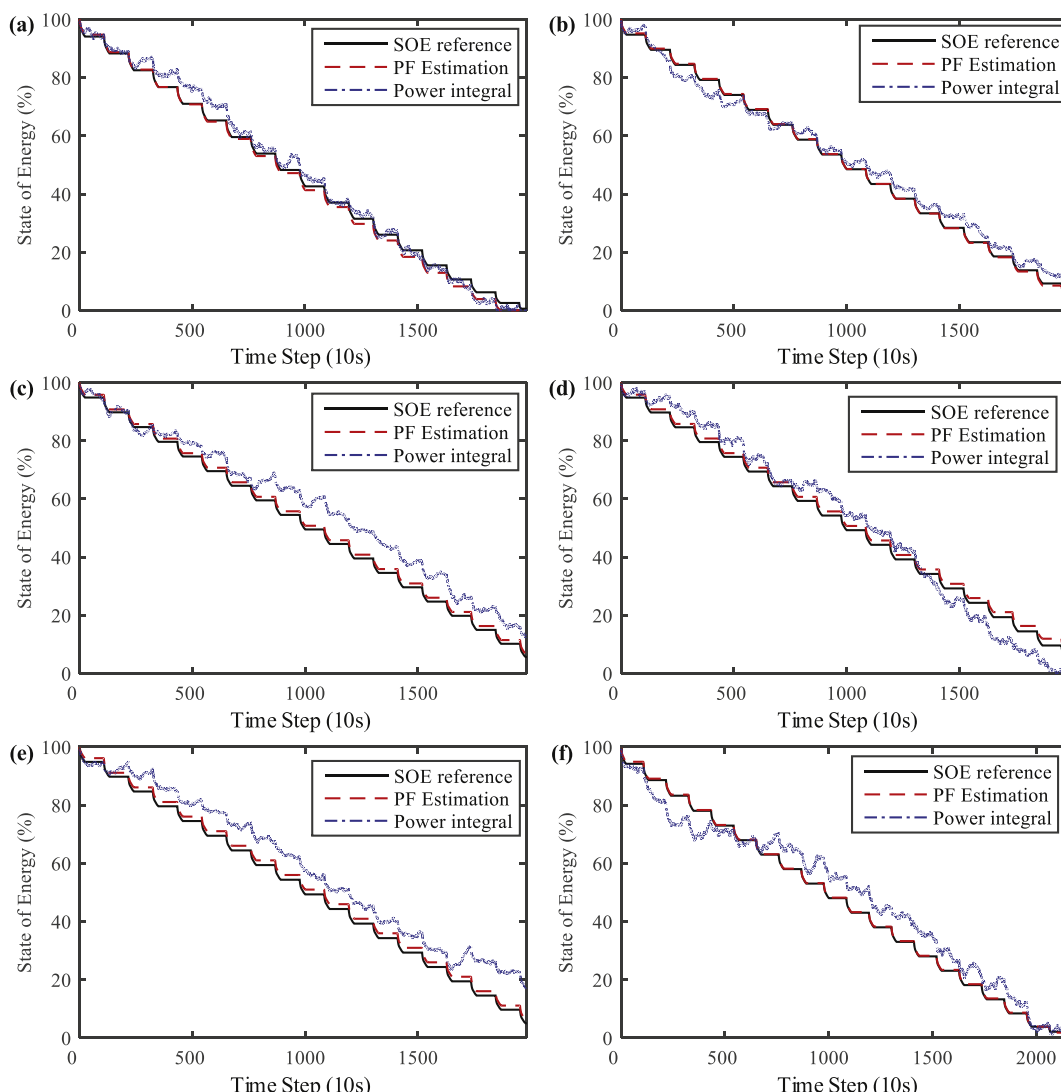


Fig. 11. SOE estimation results at different temperature conditions and dynamic discharge current after power integral and PF filtering: (a) 0 °C, (b) 10 °C, (c) 25 °C, (d) 45 °C, (e) 55 °C, (f) dynamic temperature.

Table 6

Comparison of SOE estimation under variant current using PF and power integral approach.

Temperature(°C)	RMSE (%)		MaxAE (%)	
	Power integral	Particle filter	Power integral	Particle filter
0	2.85	1.57	7.98	2.78
10	3.09	0.91	6.84	1.26
25	6.92	1.21	12.3	1.34
45	5.34	1.50	10.3	3.08
55	7.54	1.54	14.2	1.67
Dynamic temperature	5.93	1.05	11.1	1.61

show that the proposed WNN–PF SOE estimation method provides a good robustness with dynamic current at different temperatures.

The above comparison results show that the proposed method based on the PF can suppress the measurement noises and provide better performance for SOE estimation. Meanwhile, when the battery is loaded under various current conditions at different temperatures, the proposed method based on the WNN–PF also provides a good estimation accuracy, which indicates that the proposed method provides a good robustness.

6. Conclusions

Battery residual energy which provides the essential basis of energy deployment, load balancing, and security of electricity for the complex energy systems, is an important evaluation index for energy optimization and management of power battery systems. For achieving accurate estimation, the main work can be summarized: (1) In considering that the state of charge cannot indicate the energy state of battery. The state of energy, instead of state of charge, is introduced to describe the energy state of battery. (2) Resulting from the uncertain discharge rate and dynamic temperature of battery cell, it is hard to solve the nonlinear problem between state of energy and terminal voltage, and to accurately quantify the model parameters with the archived measured data. To address this issue, a wavelet neural network based battery state-space model is proposed. The temperature and discharge rate are also taken into account to improve model accuracy. Experimental results show that the proposed wavelet neural network based model provides good prediction performance. (3) A particle filter is employed to develop the estimator for state of energy. The robustness of the proposed method has been verified against different operating temperatures and discharge currents. The results on LiFePO₄ batteries indicate that the proposed method can improve the accuracy and robustness of the state of energy estimation within an error of $\pm 4\%$. To reduce the hardware cost, the complexity of the proposed algorithm needs to be further decreased in future studies.

Acknowledgments

This work was supported by the National Natural Science Fund of China (Grant No. 61375079).

References

- Zou Y, Hu X, Ma H, Li SE. Combined state of charge and state of health estimation over lithium-ion battery cell cycle lifespan for electric vehicles. *J Power Sources* 2015;273:793–803.
- Hu C, Jain G, Tamirispa P, Gorka T. Method for estimating capacity and predicting remaining useful life of lithium-ion battery. *Appl Energy* 2014;126:182–9.
- Kang J, Yan F, Zhang P, Du C. Comparison of comprehensive properties of Ni-MH (nickel-metal hydride) and Li-ion (lithium-ion) batteries in terms of energy efficiency. *Energy* 2014;70(1):618–25.
- Hu X, Li SE, Jia Z, Egardt B. Enhanced sample entropy-based health management of Li-ion battery for electrified vehicles. *Energy* 2014;64(1):953–60.
- Fathabadi H. High thermal performance lithium-ion battery pack including hybrid active–passive thermal management system for using in hybrid/electric vehicles. *Energy* 2014;70(1):529–38.
- Liu X, Wu J, Zhang C, Chen Z. A method for state of energy estimation of lithium-ion batteries at dynamic currents and temperatures. *J Power Sources* 2014;270:151–7.
- Waag W, Sauer DU. Adaptive estimation of the electromotive force of the lithium-ion battery after current interruption for an accurate state-of-charge and capacity determination. *Appl Energy* 2013;111:416–27.
- Hausmann A, Depciuk C. Expanding the Peukert equation for battery capacity modeling through inclusion of a temperature dependency. *J Power Sources* 2013;235:148–58.
- Shen WX. State of available capacity estimation for lead-acid batteries in electric vehicles using neural network. *Energy Convers Manag* 2007;48(2):433–42.
- Liu X, Wu J, Zhang C, Chen Z. Available capacity estimation of electric vehicle batteries based on Peukert equation at various temperatures. *Appl Mech Mater* 2014;535:167–71.
- Wang F, Chen J, Tan Z, Wu M, Yi B, Su W, et al. Low-temperature electrochemical performances of LiFePO₄ cathode materials for lithium ion batteries. *J Taiwan Inst Chem Eng* 2014;45(4):1321–30.
- Yi J, Kim US, Shin CB, Han T, Park S. Modeling the temperature dependence of the discharge behavior of a lithium-ion battery in low environmental temperature. *J Power Sources* 2013;244:143–8.
- Ng KS, Moo C-S, Chen Y-P, Hsieh Y-C. Enhanced coulomb counting method for estimating state-of-charge and state-of-health of lithium-ion batteries. *Appl Energy* 2009;86(9):1506–11.
- Sun F, Hu X, Zou Y, Li S. Adaptive unscented Kalman filtering for state of charge estimation of a lithium-ion battery for electric vehicles. *Energy* 2011;36(5):3531–40.
- Liu X, Chen Z, Zhang C, Wu J. A novel temperature-compensated model for power Li-ion batteries with dual-particle-filter state of charge estimation. *Appl Energy* 2014;123:263–72.
- Zhong L, Zhang C, He Y, Chen Z. A method for the estimation of the battery pack state of charge based on in-pack cells uniformity analysis. *Appl Energy* 2014;113:558–64.
- He Y, Liu X, Zhang C, Chen Z. A new model for state-of-charge (SOC) estimation for high-power Li-ion batteries. *Appl Energy* 2012;101:808–14.
- Charkhgard M, Farrokhi M. State-of-charge estimation for lithium-ion batteries using neural networks and EKF. *IEEE Trans Ind Electron* 2010;57(12):4178–87.
- Salkind AJ, Fennie C, Singh P, Atwater T, Reisner DE. Determination of state-of-charge and state-of-health of batteries by fuzzy logic methodology. *J Power Sources* 1999;80:293–300.
- Alvarez Anton JC, Garcia Nieto PJ, Blanco Viejo C, Vilan Vilan JA. Support vector machines used to estimate the battery state of charge. *IEEE Trans Power Electron* 2013;28(12):5919–26.
- Stockar S, Marano V, Canova M, Rizzoni G, Guzzella L. Energy-optimal control of plug-in hybrid electric vehicles for real-world driving cycles. *IEEE Trans Veh Technol* 2011;60(7):2949–62.
- Mamadou K, Lemaire E, Delaille A, Riu D, Hing SE, Bultel Y. Definition of a state-of-energy indicator (SOE) for electrochemical storage DEVICES: application for energetic availability forecasting. *J Electrochim Soc* 2012;159(8):A1298–307.
- Kermani S, Trigui R, Delprat S, Jeanneret B, Guerra TM. PHIL Implementation of energy management optimization for a parallel HEV on a predefined route. *IEEE Trans Veh Technol* 2011;60(3):782–92.
- Wang Y, Zhang C, Chen Z. A method for joint estimation of state-of-charge and available energy of LiFePO₄ batteries. *Appl Energy* 2014;135:81–7.
- Zhang W, Shi W, Ma Z. Adaptive unscented Kalman filter based state of energy and power capability estimation approach for lithium-ion battery, vol. 289; 2015. p. 50–62.
- Guenther C, Schott B, Hennings W, Waldowski P, Danzer MA. Model-based investigation of electric vehicle battery aging by means of vehicle-to-grid scenario simulations. *J Power Sources* 2013;239:604–10.
- Jun Z, Walter GG, Miao Y, Wan Ngai Wayne L. Wavelet neural networks for function learning. *IEEE Trans Signal Process* 1995;43(6):1485–97.